E≋RS

Bonding of zirconia to super alloy with the active brazing technique

D. Sciti, A. Bellosi, L. Esposito *

CNR-IRTEC, Research Institute for Ceramics Technology, Via Granarolo 64, Faenza, Italy

Abstract

Zirconia stabilized with yttria was bonded to a Ni-based superalloy by active brazing. An interlayer with the composition of the silver–copper eutectic plus 1.75 wt.% titanium was used as brazing material. Various brazing heating cycles were performed using a furnace with graphite heating elements and under flowing argon. The microstructure of the bonded couples is related to the chemical reactions occurring during the brazing cycles, to the properties of the specific compounds formed and to the interdiffusion phenomena occurring across the interfaces. Critical feature for the success of the joint is the nature of the interfaces that the brazing interlayer formed with the superalloy and the zirconia. At the interface with the superalloy adhesion is obtained under a relatively wide range of experimental conditions. On the contrary, at the interface with zirconia, a good wetting and adhesion occurred only when a titanium oxide sublayer with a specific thickness formed. The best results were obtained with a maximum temperature between 870 and 900°C, a soaking time of 10 min and a fast heating rate (10°C/min). The optimal thickness of the TiO_x sublayer was less than 1 μm. © 2000 Elsevier Science Ltd. All rights reserved.

Keywords: Bonding; Brazing; Interfaces; Joining; Microstructure-final; Ni alloy; ZrO_2

1. Introduction

Zirconia is an important structural material because of its high fracture toughness and strength.[1] These properties are beneficial in many practical applications, that often require the ceramic to be bonded to a metal (pure, steel or alloy).[2–8] One of the more appealing fields of interest for the use of zirconia is represented for example by gas turbines.[9–12] Superalloy components are typically used for these applications. They are usually coated with a thin layer of zirconia with the technique of plasma spraying in order to increase the maximum operating temperature of the components.[10,11] The weak feature of such thermal barrier coatings is the residual porosity and the low adhesion of the coating to the superalloy that promotes its spalling.[12] An alternative is to use dense zirconia components for the hot zone of the turbine strongly bonded at one end to the superalloy. The advantage of such a design is the high temperature performance of dense zirconia under aggressive conditions coupled with the mechanical strength of the superalloy. In addition the temperature at

the ZrO_2-superalloy interface is lower if a thick ceramic substrate is used instead of a china coating. A tight and reliable bond between the ceramic and the superalloy is the key factor for the success of the overall engine as well as for several other industrial applications.

Various techniques can be proposed to bond zirconia to metallic materials.[13–17] Among these, brazing is flexible and relatively simple.[18–20] Brazing is typically performed with a metallic interlayer, which at the melting temperature promotes the bonding by wetting and eventually reacting with the two materials. One of the advantages of this technique is the possibility to choose the interlayer among a wide variety of different compositions, according to the specific physico-chemical characteristics of the materials.

Commercial brazing materials are generally systems Ag–Cu, Ag–Cu–Ti, Ag–Cu–Sn–Ti, Ag–Cu–In–Ti, Ti, etc.[2,7,18,20] The eutectic composition of the system Ag–Cu (mp 780°C) is often preferred because it is relatively ductile and therefore able to limit the stresses arising between two materials with different thermal expansion coefficients.

The success of a brazing process depends in the first place on the ability of the interlayer to wet the two materials. In the case of ceramic-alloy bonds, the

---

* Corresponding author.

E-mail address: irtec@irtec1.irtec.bo.cnr.it (L. Esposito).

ceramic is often poorly wet. To improve the wetting a small amount of an 'active' element can be added to the composition of the interlayer. Elements like titanium or zirconium lower drastically the contact angle with the ceramic and in addition improve the adhesion by reacting with the oxide that constitutes the main phase of the ceramic. In the case of alumina for example, the contact angle decreases from 130° to 20° with the addition of titanium (1 wt.%) to the Ag–Cu eutectic composition.[7,8] Although the reduction of Al_2O_3 by titanium is generally thermodynamically unfavored, in the presence of specific molten alloys or in the case of the formation of Ti_3Al, substoichiometric TiO_x compounds can form at the interface. [21–23]

The reactivity of titanium and the nature of the new compounds depend on the specific system and experimental conditions, in particular the oxygen partial pressure in the furnace chamber. The oxygen in fact may promote the formation of a brittle compound at the interface which weakens the bond instead of promoting the adhesion. Titanium also changes the melting point of the brazing alloy and causes the liquidus and solidus separation so that during melting a transitional two-phase stage easily occurs, which leads to the stiffening and hardening of the joint.[5,20,24]

These represent some of the possible side effects that must be carefully evaluated and controlled for the production of reliable and strong joints. The following processing parameters play a key role during the joining process: amount of active element, heating cycle (heating rate, maximum temperature and soaking time) and furnace atmosphere. The properties of the starting ceramic material affect the bonding quality as well. For example, ZrO_2 stabilized with Y_2O_3 or MgO is readily wet and strongly bonded by Ag–Cu based brazing alloys containing various amounts of titanium whereas zirconia stabilized with ceria exhibits a poor wetting under the same processing conditions.[5,15]

In this work, the brazing technique is applied to bond dense, yttria tetragonal stabilized zirconia to a Ni based alloy. This particularly refractory alloy is selected because it is used for turbine components and has a coefficient of thermal expansion close to that of zirconia. The selected braze interlayer has the composition of the Ag–Cu eutectic plus 1.75 Ti. As it melts at relatively low temperature, brazing cycles can be performed in the temperature range of 800–900°C. The influence of some critical experimental parameters on the characteristics of the joints is discussed with particular emphasis on the microstructural features of the interface affecting wetting and adhesion.

2. Experimental procedure

The materials used in this work are:

- *Tetragonal stabilized ZrO_2*: Zirconia powder containing 3 mol% of yttria (TZ3Y, Toyo Soda, Japan) was used to produce fully dense discs (6.05 g/cm^3) by cold isostatic pressing and pressureless sintering (1500°C for 1 h). The thermal expansion coefficient (α) of this material is $10 \times 10^{-6}/°C$.
- *Alloy Inconel 738*: This is a Ni-based superalloy with a solidus and liquidus temperature of 1230 and 1315°C, respectively. The chemical composition and the properties of this material are reported in Table 1.[25]
- *Brazing interlayer Cusil ABA* (Wesgo, Inc., Belmont CA): The composition (63.00 Ag–35.25 Cu–1.75 Ti wt.%) corresponds to the Cu–Ag eutectic, which occurs at 780°C, plus the titanium. The softening temperature ranges between 780 and 815°C. The principal chemical and physical properties are reported in Table 1. Very thin foils (50 μm), easy to handle and cut, are used.

Table 1
Chemical composition and relevant physical and mechanical properties of the alloy Inconel IN 738[25] and of the brazing alloy Cusil ABA

Material	Cusil ABA[a]	Inconel IN738[b]
Chemical composition (wt.%)	Ag 63.00; Ti 1.75; Cu bal.	C 0.17; Cr 17.00, Co 8.50; Mo 1.75; W 2.60; Ta 1.75; Nb 0.90; Al 3.4; Zr 0.10; B 0.01; Ni bal
Solidus temperature	780°C	1230°C
Liquidus temperature	815°C	1315°C
Density	9.8 g/cm^3	8.11 g/cm^3
Thermal conductivity	180 W/mK	17.7–27.2 W/m K from 538 to 1093°C
Coefficient of thermal expansion α (from RT to 500°C)	$18.5 \times 10^{-6}/K$	$11.6–14.0 \times 10^{-6}/K$
Young's modulus	83 GPa	201–175 GPa from RT to 538°C
Yield strength	271 MPa	950 MPa
Ultimate tensile strength	346 MPa	1095 MPa

[a] Supplied by Wesgo Inc., Belmont, Ca.
[b] Supplied by Ansaldo Ricerche, Genova, Italy.

For the brazing tests, slices of ZrO_2 and superalloy ($15\times15\times2$ mm^3), were used. One flat surface of each was polished up to 1 µm with diamond paste. The brazing foil was cut into slices (15×15 mm^2). The three materials were ultrasonically cleaned in acetone and then ethanol for about 10 min each. Finally they were assembled together with the polished surfaces in direct contact tol the brazing interlayer, as shown in Fig. 1. The sandwich was then placed inside a grafite crucible and protected by a powder bed containing 80 wt.% of Al_2O_3 and 20 wt.% Al as oxygen gatter. A furnace with graphite heating elements and flowing argon atmosphere were used for all the brazing cycles. The argon was not gettered and therefore contained also some oxygen (less than 2 ppm). The oxygen partial pressure was less than 2×10^{-1} Pa.

Two sets of brazing cycles were performed (Table 2), with the following processing parameters:

- *Set I*: Heating (10°C/min) up to 780°C (the solidus temperature of the brazing interlayer). This temperature was maintained for 20 min, then the maximum temperature was reached with a slow heating rate (2°C/min) and kept for 1 min.
- *Set II*: Heating (10°C/min) up to the maximum temperature. Soaking time in the range 10–30 min.

For both sets the cooling rate was 2°C/min to 700°C and then about 10°C/min.

No weight change of the samples occurred during the thermal treatments.

Interfacial microstructure and microchemistry were analyzed by scanning electron microscopy (SEM) and energy dispersive spectroscopy (EDS) on polished cross sections. X-ray diffractometry was used to analyze the surfaces of those samples that were in contact during the brazing cycle but failed during the cutting operations.

3. Results

The heating schedule and characteristics of the processed samples are reported in Table 2. The brazing interlayer formed two interfaces, one with the superalloy and the other with the zirconia.

Adhesion at the interface between the brazing interlayer and the superalloy was obtained in all the samples. Conversely, adhesion at the interface zirconia-brazing interlayer depended on the heating schedule. This interface was fractured or poorly bonded in all the samples of set
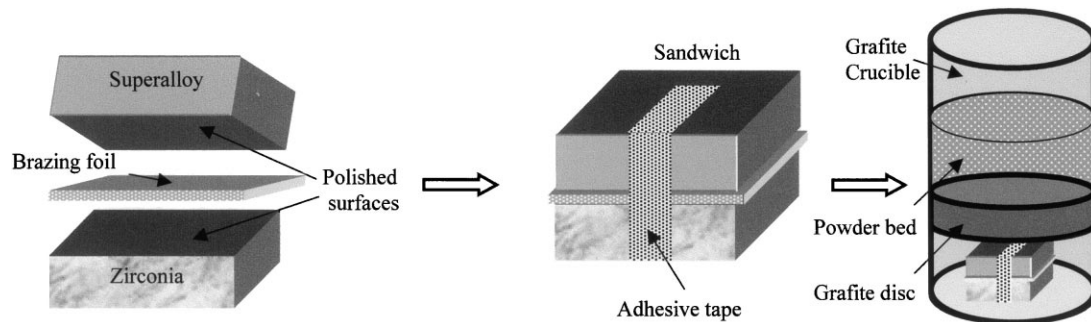

Fig. 1. Flow chart of the procedure used to assemble the samples.

Table 2
Brazing cycles performed on ZrO_2/Cusil ABA/Inconel 738 samples

Set	No.	Holding step (°C×min)	Heating rate after hold step (°C/min)	Brazing cycle (°C×min)	Final Cusil layer (µm)	Final Ti,Cu,Ni, sublayer (µm)	Final TiO_x sublayer (µm)	Adhesion at the interface
I	1	780×20	2	820×1	50	2–3	No layer	No
	2	780×10	2	833×1	a	a	a	No
	3	780×20	2	850×1	30	3–4	No layer	Partial
	4	780×20	2	900×1	a	a	a	Partial
	5	780×20	2	950×1	a	a	a	No
II	6	None	10	850×30	a	a	a	No
	7	None	10	870×10	50	No layer	0.6	Yes
	8	None	10	870×30	40	No layer	0.8	Yes
	9	None	10	900×10	35	5–10	1.2	Yes
	10	None	10	920×10	30–90	a	a	Partial
	11	None	10	940×10	a	a	a	No

^a The final thickness could not be measured.

I subjected to the holding step at 780°C. In the samples that quickly reached the maximum temperature (set II) the adhesion depended on the temperature itself and on the holding time. The optimal temperature ranged between 870 and 900°C, while at lower and higher temperatures the adhesion was partial or absent and the samples fractured when handled or cut.

Despite the differences in the heating schedule some common features were observed in all the samples:

- *The brazing interlayer thickness decreased during the heating cycle as a function of the maximum temperature.* (Table 2, Figs. 2 and 3). In samples of set II with a constant holding time of 10 min, the thickness decreased down to a minimum value of 35 µm at 900°C. At higher temperature the interlayer partially squeezed out of the interface because of its decreased viscosity. As a consequence, its thickness became irregular: for example, in sample 10, treated at 920°C, the filler metal thickness varied from 30 to 90 µm. The soaking time had probably similar influence: the final thickness of Cusil in sample 8, treated for 30 min at 870°C, was 10 µm less than in sample 7, treated for 10 min at the same temperature.

- *The brazing interlayer separated to form two phases, one rich in silver and the other in copper* (light and dark gray, respectively, in the SEM pictures; Figs. 2 and 3). The eutectic solidification structure of the braze was different when cooled from different temperatures, i.e. a fine structure with relatively small copper "islands" when cooled from temperatures just above the liquids to a very coarse structure when cooled from 900°C (compare for example (Fig. 2a and 3c). Traces of titanium were found in both of these phases.

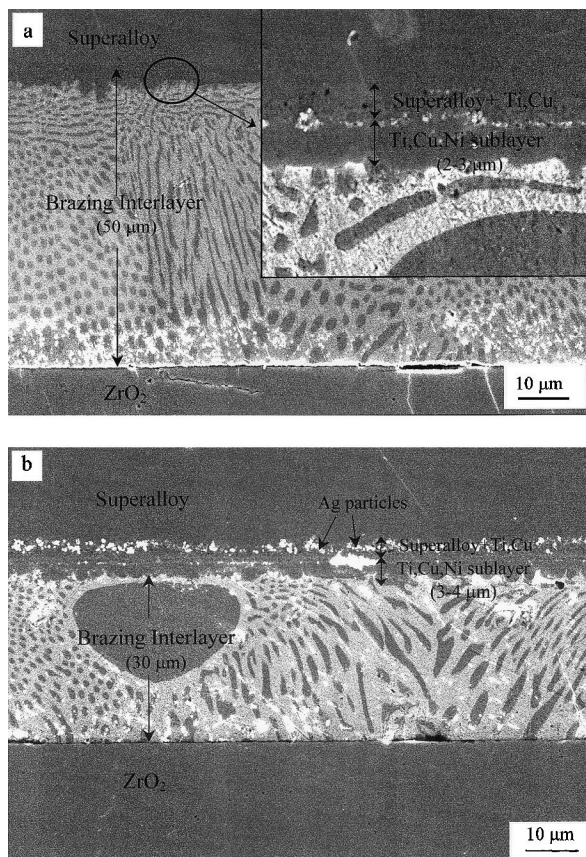Fig. 2. Cross-section of samples 1 (a) and 3 (b) (set I, Table 2). Layer I contains Ti, Cu and Ni in similar amounts (at.%). Layer II is formed by Inconel IN738 enriched with titanium (about 10 at.%) and copper (about 4 at.%).
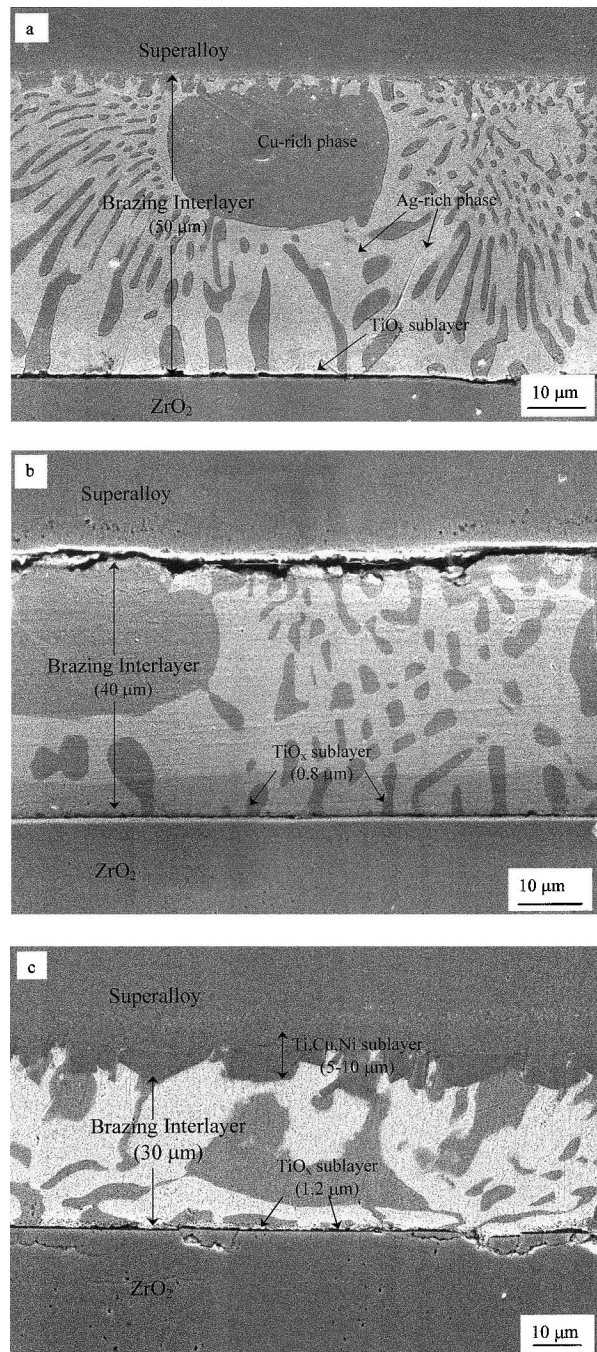

Fig. 3. Cross-section of samples (a) 7, (b) 8 and (c) 9 (set II, Table 2).

- *The main elements interdiffused among the materials.* Titanium migrated at both the interfaces, silver and copper diffused toward the superalloy and some elements of the superalloy diffused across the brazing interlayer toward the interface with ZrO_2. At this interface quantitative microanalysis revealed concentrations as high as 20 at.% of Ni and 10 at.% of Cr and also traces of Co and Al. The concentration profiles of Ti and Ni along the cross-section are shown in Fig. 4.

In samples 7–9 the quality of the adhesion was assessed with a Vickers indenter with 10 kg load. The indentation was perfomed on zirconia about 50 μm far from the interface (see the subset in Fig. 5). The crack that developed perpendicular to the interface did not propagate along the interface or into the brazing interlayer (Fig. 5). The latter deformed plastically as a consequence of the stresses induced by the crack (i.e. along the interface), so that the crack opening displacement was larger at the interface than at the indentation corner. The residual stresses at the interface also affected the cracks that formed at the opposite corners of the indentation in the direction parallel to the interface. In fact, since $\alpha_{ceramic} < \alpha_{metal}$, compressive stresses developed along the interface on the ceramic side and tensile stresses on the metal one.[26] As a consequence the cracks were oriented toward the interface, and did not follow a straight line. Due to the absence of the crack propagation across the interface, no numerical information can be obtained on the strength of the joint. However, as a preliminary result, it must be mentioned that the shear stresses induced by the crack at the interface actually did not cause the failure of the joint.

In the following sections the specific features of the two interfaces will be separately described.

3.1. Superalloy–brazing material interface

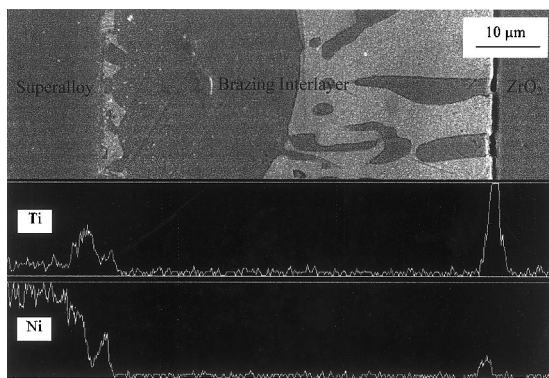As previously mentioned, at the interface between the superalloy and the filler metal a good adhesion with no crack or pore was easily obtained (Figs. 2 and 3a), but differences exist between the two sets of samples (Table 2).

In the samples where the maximum temperature was reached after a step of 20 min at 780°C (set I) titanium migrated in a massive amount to this interface, in some cases up to about 30 at.%. Here it formed one or even two distinct sublayers with the other elements of the brazing interlayer and of the superalloy as indicated in Fig. 2.. Ti, Ni, and Cu were found in equal amounts in the sublayer closer to the brazing material. The thickness of such sublayers increased with temperature. The second sublayer had a composition similar to the superalloy but with a higher titanium content and some copper; it did not form a sharp interface on the alloy side and contained dispersed particles of silver.

Sample 7, set II, was treated at higher temperature and longer time (870°C, 10 min) than samples 1 and 3, set I (820 and 850°C, respectively, and 1 min), but no distinct sublayer was revealed at the interface (Fig. 3a). Here, only a slight diffusion of copper and titanium from the filler metal toward the alloy and the precipitation of silver particles occurred, as revealed by the element profiles of the cross-section (Fig. 6). Such a diffuse sublayer is similar to the above described second sublayer present in samples 1 and 3 (Fig. 2). At higher temperature (900°C, sample 9) a sublayer containing Ti, Cu and Ni (i.e. similar to the first sublayer of samples 1 and 3) was observed (Fig. 3c). The thickness of this sublayer increased with temperature whereas the thickness of the residual filler metal decreased (Table 2).

3.2. Zirconia–brazing material interface

The interface between ZrO_2 and the brazing material was fractured or contained numerous pores in all the samples of set I (Fig. 2). The X-ray patterns of the two open surfaces that were in contact during the heating cycle did not repeat any new compound.

On the contrary complete adhesion was obtained in samples 7–9 of set II (Table 2), treated, respectively, at 870°C for 10 and 30 min and at 900°C for 10 min (Fig. 3).

Fig. 4. Interface between ZrO_2 and Cusil after the indentation test with a Vickers indenter using 10 kg load on sample 7.
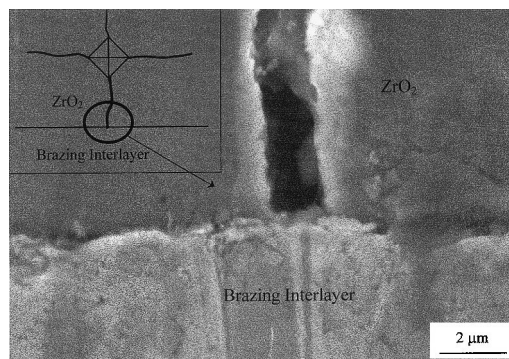

Fig. 5. Cross-section of the bonded region of sample 7 and the EDS profiles of nickel and titanium.

In all the samples of set II, two sublayers were revealed by the EDS profile of the elements (Figs. 4 and 7):

TiO$_x$ sublayer: sublayer containing titanium and oxygen formed at the interface with ZrO$_2$ (X-ray diffractiometry could not be conducted on such bonded samples). Although it was not possible to determine experimentally its exact stoichiometry, it should range between those of TiO and TiO$_2$. The free energy of formation of these compounds is in fact negative in the temperature range tested. Since the P$_{O_2}$ required for the TiO$_2$ reduction is several order of magninitude smaller than the P$_{O_2}$ in the furnace (2×10^{-1} Pa),[27] this oxide should form and be stable at the interface. Indeed, other factors may affect the Ti reaction, for example, when the brazing interlayer melts and wets the ZrO$_2$ and the superalloy, Ti is not in direct contact with the atmosphere of the furnace, therefore oxidation may be inhibited. Moreover, oxygen contained in the flowing argon partially reacts with the Al powder contained in the powder bed and therefore the P$_{O_2}$ close to the inter-

layer should be less than 2×10^{-1} Pa. Consequently, the stoichiometry of the observed TiO$_x$ sublayer can be different depending on the specific experimental condition, in particular the maximum temperature and the soaking time. The thickness of the TiO$_x$ sublayer is very limited, varying with temperature from 0.6 (sample 7) to 1.2 μm (sample 9), as shown in Fig. 8. At temperatures higher than 900°C, the TiO$_x$ sublayer did not grow homogeneously along the entire interface. In these cases (samples 10 and 11) the adhesion was poor and the samples fractured at this interface during the handling operations.

Ti, Ag, Ni sublayer: The second sublayer that formed at this interface contains mainly Ti, Ag, Ni and traces of Cr (Figs. 7 and 8a). Its formation was particularly evident in sample 7 (870°C/10min), as revealed in Fig. 7 by the SEM-EDS analysis. At 900°C or at higher temperature the Ti, Ag, Ni sublayer did not grow homogeneously along all the interface (Fig. 8b). In particular, when the zirconia was in contact with the region of the interlayer rich in Ag, also the Ni and Cr amounts in the second sublayer were higher.
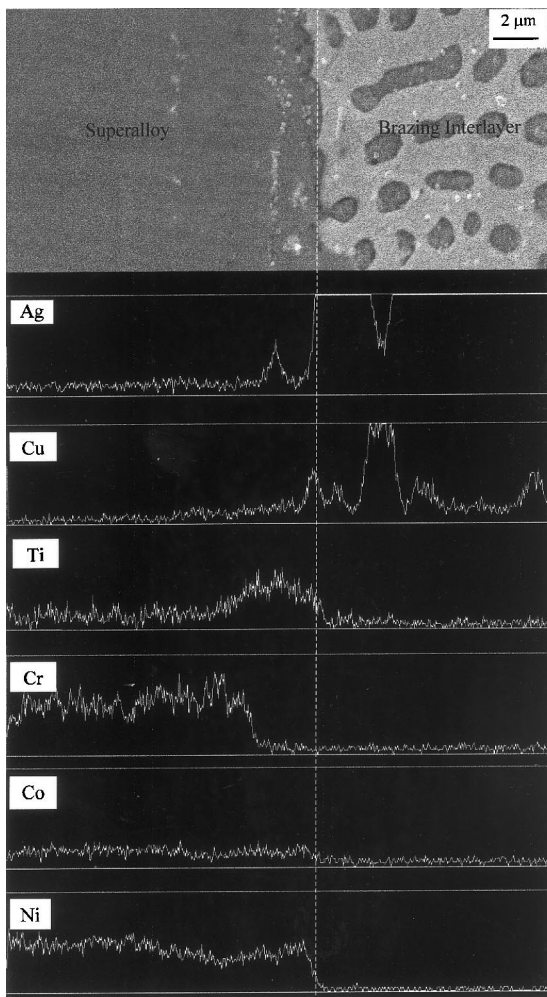

Fig. 6. Interface Inconel IN738/Cusil ABA of sample 7 (Table 2) and related EDS concentration profiles of the elements (qualitative).
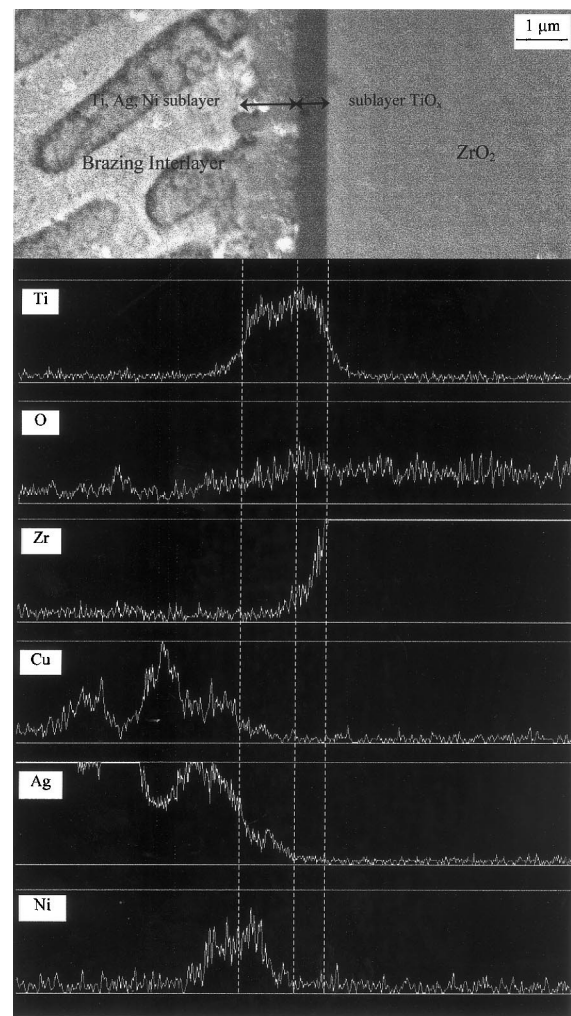

Fig. 7. Interface Cusil ABA/ZrO$_2$ of sample 7 (Table 2) and related EDS concentration profiles of the elements (qualitative).
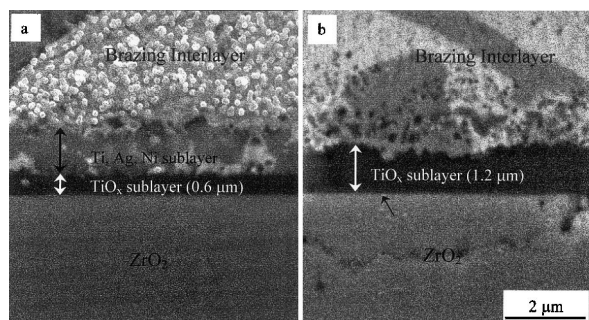
Fig. 8. Interface Cusil/ZrO_2 of sample (a) 7 and (b) 9 and related TiO_x sublayers.

Conversely, where zirconia was in contact with a Cu rich area, the sublayer was thinner or absent.

In order to determine the possible presence of new phases, the half of the fractured joint of sample 11, set II, (Fig. 9) was analyzed through the X-ray diffractometry. The X-ray pattern did not reveal the presence of titanium oxide, probably because it was too thin, but showed traces of $TiAg_3$, probably within the Ti, Ag, Ni sublayer that formed in these samples.

4. Discussion

The brazing cycles performed have shown that adherent joints can be obtained between zirconia and superalloy and that the critical step of the overall process is to realize a good adhesion at the interface between zirconia and the brazing material. This goal is accomplished when a thin layer of titanium oxide form at such interface, and this occurs under specific experimental conditions: fast heating rate, temperature between 870 and 900°C and soaking time of 10 min. The thickness and homogeneity of this layer are the key factors for the success of the joint and under these conditions a adherent TiO_x layer with a thickness of 0.6–1.2 μm forms at the interface with ZrO_2.
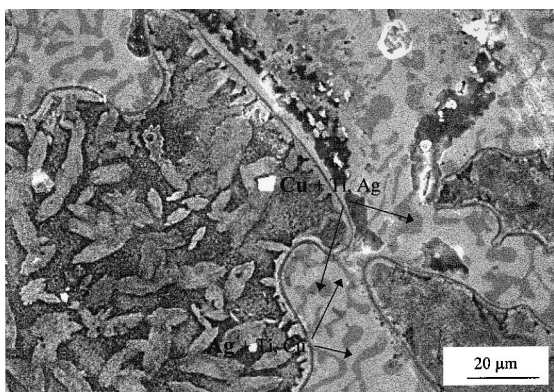

Fig. 9. Microstructure of the fractured surface of the Inconel side of sample 11 (Table 2).

The evolution of the TiO_x layer depends also on the formation of another layer containing Ag and Ti and probably compounds as $TiAg_3$. In fact, once a thin TiO_x sublayer formed, the production of a second sublayer was probably favoured compared to the oxidation of titanium. This sublayer also contains elements as Ni and Cr that diffused from the superalloy across the brazing material. The presence of these elements probably enhanced the formation of such sublayer.

As previously described, poor or no adhesion was obtained when the samples were held at 780°C for 20 min. Such holding step may have promoted the migration of titanium preferentially at the interface with the superalloy. As a consequence the TiO_x sublayer did not form at the interface with zirconia and there was no adhesion. The preferential titanium migration toward the superalloy could be driven by the concurrent migration of nickel to the same interface (Fig. 2).

No adhesion was obtained when samples were treated at $T > 900$°C (samples 10 and 11, Table 2). In these cases the titanium migration within the brazing interlayer toward the zirconia was probably faster compared to lower temperatures. Moreover, the lower viscosity of the brazing alloy hastened its separation in the Ag and Cu-rich regions within the residual brazing interlayer during cooling (Fig. 3c). Hence, titanium migrated fast toward zirconia and formed a thick titanium oxide layer. The failure of these joints may be driven by several features. One is that a thick TiO_x sublayer is less resistant to the tensile stresses arising between the ZrO_2 and the superalloy during cooling. Another feature is the stoichiometry of the TiO_x sublayer. Previous studies on the brazing of Al_2O_3 have shown that the stoichiometry of the titanium oxide affects the strength of the joint.[7,8,28] The stoichiometry ranges between TiO, a metallic compound characterized by a high wettability, to TiO_2, a ceramic compound with a lower wettability. The relatively high PO_2 of the adopted experimental conditions, together with the faster titanium migration, could have promoted and hastened the formation of titanium oxides with higher oxygen contents, i.e. Ti_2O_3, Ti_3O_5 or eventually TiO_2.[29] Once formed, such compounds drove the failure of the joint because they are brittle; their wettability is poor and therefore they cannot accommodate the thermal expansion mismatch between the ceramic and the superalloy.

In the literature on the brazing of alumina[7,18] the formation of TiO_x layers at the interface is often considered the consequence of the reduction of Al_2O_3 by titanium. Under the experimental conditions used, however, such reaction is not thermodynamically favored. The energy needed to produce an equal amount of zirconium is even higher. In the present case, the observed formation of TiO_x compounds is more probably the consequence of the reaction of titanium migrated at the interface with the residual oxygen present in the atmosphere. Such mechanism of reaction explains why, after the brazing cycles,

the surface of ZrO_2 in contact with the brazing interlayer is still smooth and straight (Fig. 3). In fact, if ZrO_2 had reacted with Ti the surface would have been irregular, as shown in the case of the reaction of Al_2O_3 with Ti.[23]

5. Conclusions

Successful joints characterized by a good wetting and adhesion between zirconia partially stabilized with yttria and a Ni-based superalloy (Inconel IN 738) were obtained using a Cu, Ag, Ti brazing interlayer (Cusil ABA). Titanium is the active element of this system and its diffusion and reaction drove the overall process. Under specific experimental conditions (fast heating rate of 10°C/min, maximum temperature between 870 and 900°C and a soaking time of 10 min) a homogeneous TiO_x layer with a limited thickness formed at the interface between zirconia and the brazing interlayer. Such layer was assessed to be the key factor for the adhesion at this interface. At the other interface between the brazing interlayer and the superalloy adhesion with no pore and limited interdiffusion of the involved elements was obtained under a wider range of experimental conditions. The consequent good wetting and adhesion between the two materials promoted the formation of reliable joints as confirmed by the Vickers indentation tests.

Acknowledgements

References

1. Butler, E. P., Transformation-toughened zirconia ceramics. *Mat. Sci. Techn.*, 1985, **1**, 417–432.
2. Mizuhara, H. and Oyama, T., Ceramic/metal seals. In: *Engineered Materials Handbook, Ceramic and Glasses*. Vol. 4, ed. H. F. Lampman and N. D. Wheaton. ASM International, USA, 1991, pp. 502–510.
3. Suganuma, K., Recent Advances in joining technology of ceramics to metals, review. *ISIJ International*, 1990, **30**(12), 1046–1058.
4. Peteves, S. D., Paulasto, M., Ceccone, G. and Nicholas, M. G., Ceramic/metal reactions and microstructures in ceramic joints. In *Ceramic Microstructure: Control at the Atomic Level*, ed. A. P. Tomsia and A. M. Glaeser. Plenum Press, New York, 1998, pp. 359–369.
5. Moorhead, A. J. and Kim, H.-E., Joining oxide ceramics. In: *Engineered Materials Handbook, Ceramic and Glasses*. Vol. 4, ed. H. F. Lampman and N. D. Wheaton. ASM International, USA, 1991, pp. 511–522.
6. Suganuma, K., Joining non-oxide ceramics. In: *Engineered Materials Handbook, Ceramic and Glasses*. Vol. 4, ed. H. F. Lampman and N. D. Wheaton. ASM International, USA, 1991, pp. 523–531.
7. Tomsia, A. P. and Loehman, R. E., Reactions and micro-structure at selected ceramic/metal interfaces. *Mat. and Manufact. Processes*, 1994, **9**(3), 547–561.
8. Tomsia, A. P., Saiz, E., Foppiano, S. and Cannon, R. M., Reactive wetting in ceramic/metal systems. In *Proceedings of the 9th Cimtec—World Ceramics Congress, Ceramics: Getting into the 2000's–Part C*, ed. P. Vincenzini. Techna srl, Italy, 1999, pp. 913–926.
9. Meier, S. M. and Gupta, D. K., The evolution of thermal barrier coatings in gas turbine engine applications. *Transactions of the ASME*, 1994, **11**(6), 250–257.
10. Alpérine, S. and Lelait, L., Microstructural investigations of plasma-sprayed yttria partially stabilized zirconia TBC (in relation to thermomechanical resistance and high-temperature oxidation mechanims. *Transactions of the ASME*, 1994, **116**, 258–265.
11. Takeuchi, Y. R. and Kokini, K., Thermal fracture of multilayer ceramic thermal barrier coatings. *Transactions of the ASME*, 1994, **116**, 266–271.
12. Newaz, G. M., Nusier, S. Q. and Chaudhury, Z. A., Damage accumulation mechanisms in thermal barrier coatings. *J. Eng. Mat. Techn.*, 1998, **120**, 149–153.
13. Iwamoto, N. and Yokoo, H., Joining of zirconia using zirconium-based alloys. *J. Mater. Sci.*, 1992, **27**, 441–447.
14. Derby, B. and Qin, C.-D., The Role of the interface in metal/ceramic diffusion bonding. In *Designing Ceramic Interfaces II*, ed. S. D. Peteves. Elsevier Applied Science, UK, 1993, pp. 389–398.
15. Colin, C., Broussaud, D., Grivon, F. and Wicker, A., Solid-state bonding of partially stabilized zirconia to metals. In *Ceramic Materials and Components for Engines*. Elsevier Applied Science, UK, 1992, pp. 492-502
16. Qin, C.-D. and Derby, B., Diffusion bonding of a nickel (chromium) alloy to zirconia: mechanical properties and interface microstructures. *J. Mater. Sci.*, 1993, **28**, 4366–4374.
17. Mun, J.-D., Derby, B. and Sutton, A. P., Texture change in Ni and Cu foils on diffusion bonding to zirconia. *Scripta Mater.*, 1997, **36**(1), 1–6.
18. Nicholas, M. G., Active metal brazing. In *Joining of Ceramics*, ed. M. Nicholas. Chapman and Hall, Great Britain, 1990, pp. 73–93.
19. Suganuma, K., Okamoto, T., Koizumi, M. and Shimada, M., Solid-state bonding of partially stabilized zirconia to steel with titanium interlayer. *J. Mat. Sci. Lett.*, 1989, **5**, 1099–1100.
20. Hao, H., Wang, Y., Jin, Z. and Wang, X., Joining of ziconia to stainless steel and to itself using $Ag_{57}Cu_{38}Ti_5$ filler metal. *J. Am. Ceram. Soc.*, 1995, **78**(8), 2157–2160.
21. Klomp, J. T. In *Ceramic Microstructures '87*, ed. J. S. Pask and A. G. Evans. Plenum Press, New York 1987, pp. 307–317
22. Beyers, R., *J. Vacuum Science and Technology*, 1984, **B2**(4), 781.
23. Li, X. L., Hillel, R., Teyssandier, F., Choi, S. K. and van Loo, F. J. J., Reactions and phase relations in the Ti–Al–O system. *Acta Metall. Mater.*, 1992, **40**(11), 3149–3157.
24. Xue, X. M., Wang, J. T. and Sui, Z. T., Wettability and interfacial reaction of alumina and zirconia by reactive silver-indium base alloy at mid-temperatures. *J. Mater. Sci.*, 1993, **28**, 1317–1322.
25. Anon., *ASM Handbook, Properties and Selection: Irons, Steels, and High Performance Alloys*, Vol. 1. ASM International, USA, 1990, pp. 981-994.
26. Jung, Y. J., Paik, U. and Choi, S. C., Influence of the particle size and phase type of zirconia on the fabrication and residual stress of zirconia/stainless-steel 304 functionally gradient materials. *J. Mater. Sci.*, 1999, **34**, 5407–5416.
27. Swalin, R. A., *Thermodynamics of Solids*. John Wiley and Sons, USA, 1962 pp. 104-118.
28. Wlosinski W. K. and Kalinski, D., Carbon fibre–AgCuTi brazing filler for metal–ceramic joining. In *The Proceedings of the 9th Cimtec — World Ceramics Congress. Ceramics: Getting into the 2000's—Part C*, ed. P. Vincenzini. Techna Srl, 1999, pp. 1027–1034
29. Massalki, T. B., *Binary Alloy Phase Diagrams*. ASM, Metals Park, OH, 1986.